Al-Azhar Bulletin of Science

Volume 34 | Issue 2 Article 6

2023
Section: Zoology

Destructive cellular and anticoagulant activities of chitosan extracted from the oriental hornet, Vespa orientalis L. (Hymenoptera: Vespidae) and the rice grasshopper, Aiolopus thalassinus (Orthoptera: Acrididae)

Ibrahim S. Ghannam
Department of Zoology, Faculty of Science, Al-Azhar University, Nasr City, Cairo, Egypt.

Mostafa I. Hassan
Department of Zoology, Faculty of Science, Al-Azhar University, Nasr City, Cairo, Egypt.

Ahmed I. Hasaballah
Department of Zoology, Faculty of Science, Al-Azhar University, Nasr City, Cairo, Egypt., ahscience09@azhar.edu.eg

Mohamed A. Awad
Department of Zoology, Faculty of Science, Al-Azhar University, Nasr City, Cairo, Egypt.

Ahmed Z.I. Shehata
Department of Zoology, Faculty of Science, Al-Azhar University, Nasr City, Cairo, Egypt.

How to Cite This Article

Ghannam, Ibrahim S.; Hassan, Mostafa I.; Hasaballah, Ahmed I.; Awad, Mohamed A.; and Shehata, Ahmed Z.I. (2023) "Destructive cellular and anticoagulant activities of chitosan extracted from the oriental hornet, Vespa orientalis L. (Hymenoptera: Vespidae) and the rice grasshopper, Aiolopus thalassinus (Orthoptera: Acrididae)," *Al-Azhar Bulletin of Science*: Vol. 34: Iss. 2, Article 6.
DOI: https://doi.org/10.58675/2636-3305.1649

ORIGINAL ARTICLE

Destructive Cellular and Anticoagulant Activities of Chitosan Extracted from the Oriental Hornet, *Vespa orientalis* L. (Hymenoptera: Vespidae) and the Rice Grasshopper, *Aiolopus thalassinus* (Orthoptera: Acrididae)

Ibrahim Saeed Ghannam, Mostafa Ibrahim Hassan, Ahmed Ibrahim Hasaballah*, Mohamed Ahmed Awad, Ahmed Zeinhom Shehata

Department of Zoology, Faculty of Science, Al-Azhar University, Nasr City, Cairo, Egypt

Abstract

The current investigation tested Chitosan isolated from adult *Vespa orientalis* and *Aiolopus thalassinus* for its cytotoxic and anticoagulant effects. Chitosan was analyzed for its effects on human breast cancer cells (MCF-7), human liver cancer cells (HepG2) and lung fibroblast cells (WI-38) after being extracted and characterized by Fourier transform infrared spectroscopy (FT-IR), X-ray diffraction (XRD) and scanning electron microscopy (SEM). Also, the anticoagulant activity of extracted chitosan using activated partial thromboplastin time (APTT) and Prothrombin Time (PT) assays was investigated. Results showed that cytotoxic activity of both extracted chitosan samples recorded cellular viability of MCF-7 cell line equal to 17.99 and 9.53% by *V. orientalis* and *A. thalassinus* extracted chitosan at 1000 μg/ml, respectively. At 500 μg/ml, the viability of the HepG2 cell line was recorded 54.95 and 20.76% by *V. orientalis* and *A. thalassinus*, respectively. In addition, *V. orientalis* and *A. thalassinus* extracted chitosan showed noncytotoxic effects against the WI-38 cell line at concentrations less than or equal to 250 and 125 μg/ml. On the other hand, the anticoagulant activity of *V. orientalis* extracted chitosan using APTT assay recorded 53.7 ± 0.01 s at 75 μg/ml, while *A. thalassinus* chitosan reached 58.91 ± 0.04 s at 75 μg/ml. While anticoagulant activity of *V. orientalis* chitosan using PT assay recorded 12.16 ± 0.07 s at 25 μg/ml, compared with 14.37 ± 0.02 s for *A. thalassinus* chitosan at the same concentration. Based on these results, can be inferred that *V. orientalis* and *A. thalassinus* may be considered as a source for chitosan with properties suitable for cytotoxic and anticoagulant activities.

Keywords: *Aiolopus thalassinus*, Anticoagulant activity, Chitosan, Cytotoxicity, *Vespa orientalis*

1. Introduction

Chitosan is a natural, nontoxic biopolymer (β-(14)-linked N-acetyl-D glucosamine) generated when the deacetylation degree of chitin (a linear chain of acetylglucosamine groups) reaches around 50.0% and becomes soluble in aqueous acidic environments. Chitosan is often used in nanoparticles, microspheres, hydrogels, films, and fibers in the biomedical and pharmaceutical industries [1–3].

An amino/acetamido group and hydroxyl groups at carbons (C) 2, 3, and 6 are all reactive functional groups in chitosan. The amino acid concentration is directly linked to their chelation, flocculation, and biological roles [4] and is the primary explanation for the diversity in their structures and physicochemical characteristics. Some structural factors,

Received 14 June 2023; revised 11 August 2023; accepted 12 August 2023.
Available online 19 September 2023

* Corresponding author at: Department of Zoology, Faculty of Science, Al-Azhar University, Nasr City, Cairo, Egypt.
E-mail address: ahscience09@azhar.edu.eg (A.I. Hasaballah).

https://doi.org/10.58675/2636-3305.1649

such as molecular weight, degree of deacetylation, distribution of both N-acetyl glucosamine and glucosamine in the polymer chain, crystallinity, and direct action against pathogens, are linked to chitosan's bioactivity [5].

However, cancer continues to be a major killer across the globe. The biology of cancer has been studied extensively in recent decades, leading to improved diagnostic and therapy options [6]. Chitosan has been shown to affect tumor cells, which may disrupt their metabolism directly, slow their development, or even cause them to self-destruct. It can fight tumors by bolstering the immune system [7,8]. Liver and breast cancers are among the most common types of cancer that are regarded as one of the main causes of mortality in both economically and developing countries [9]. MTT assay showed the inhibitory effect of chitosan prepared from the American cockroach on the proliferation of liver cancer cells (HepG2) and Breast cancer cells (MCF-7) in vitro [10].

Chitosan has been prepared from the shells of crustaceans and insects for a long time [11−16]. This process involves removing the protein, demineralization, decolorization and deacetylation. Arthropods, of which insects are a part, have inspired researchers to look for novel medicinal compounds [17−19]. The present research aimed to (1) extract, prepare and characterize chitosan from the adult *Vespa orientalis* and *Aiolopus thalassinus* (2) evaluate the cytotoxic against human breast cancer (MCF-7), human liver cancer (HepG2), and lung fibroblast cell lines (WI-38 and to (3) examine the chitosan's anticoagulant properties through activated partial thromboplastin time (APTT) and Prothrombin Time (PT) tests evaluation.

2. Materials and methods

2.1. Colonization of tested insects

2.1.1. Colonization of oriental hornet, V. orientalis

Adults of *V. orientalis* needed for the bioassay were obtained from the laboratory of the Honeybees Research Department, Plant Protection Research Institute, Dokki, Giza, Egypt.

2.1.2. Colonization of the rice grasshopper, A. thalassinus

Adults of *A. thalassinus* were collected from an insectary in the Entomology Department of Cairo University's Faculty of Science in Giza, Egypt. They were then reared in the insectary of the Animal house in the Zoology Department of Al-Azhar University (Cairo) for several generations under strictly regulated environmental conditions, including temperature (35 ± 2 °C), relative humidity (65−70%), and photoperiods (12−12 h light−dark rhythm). *A. thalassinus* were bred in wire-screen enclosures heated by electricity (40 × 40 × 50 cm). Grasshoppers were provided with fresh, clean leaves of clover (*Trifolium alexandrinum*) from November through May and subsequently with new leaves of *Sesbania sesban* from June through August. Daily cage inspections included the provision of adequate ovipositional receptacles (10 cm deep) loaded with sieved and sterilized sand that was maintained wet at all times. To prevent the eggs from drying out before they hatch, they were taken from their nests and placed in glass jars (1-L capacity), wrapped with muslin fabric, and secured with rubber bands. Grasshoppers were released into the huge cage after four or five moults, soon after hatching [20].

2.2. Chitin isolation and chitosan extraction

After adults were washed with distilled water, dried at room temperature, and then crushed in a mortar, they were pulverised. The chitin separation method used forty grammes of ground material from each insect species. The ground samples were demineralized by soaking in 400 ml of 1 M HCL for 12 h at room temperature. Next, distilled water was used to filter and rinse the samples many times. Deproteinization was performed by treating 400 ml of samples with 4 M NaOH at 90 °C for 8 h. The samples were then filtered one more and washed in distilled water. Chitin was extracted from the samples after they were decolored by passing them through a combination of chloroform, methanol, and distilled water in the ratio of (1: 2: 4) at room temperature for 6 h and then rinsing them with distilled water. Finally, chitosan was obtained by deacetylating extracted chitin at 90 °C for 8 h using 50% NaOH. Then, chitosan samples were purified by dissolving in 1% acetic acid and precipitated in 20% NaOH solution. Filtered samples were washed in distilled water to pH neutrality and dried in a dry heat sterilizer at 50 °C for 24 h [21].

2.3. Characterization of extracted chitosan

2.3.1. Solubility test

This characteristic is commonly used to preliminary identify the extracted is chitosan, the chitosan was tested for solubility in acetic acid 1% (v/v) with a ratio 1 g: 100 ml [22].

2.3.2. Fourier transform infrared spectroscopy (FT-IR)

At the Faculty of Pharmacy, Al-Azhar University in Cairo, Egypt, the produced chitosan samples were analyzed by Fourier transform infrared spectroscopy (FT-IR) using a JASCO FT-IR-6200 apparatus. We used Akila's approach [23] to determine the chitosan degree of deacetylation (DDA) as follows.

$$DDA\% = 100\text{-}\ [(A_{1655}/\ A_{3450}) \times 100/1.33]$$

Where: A_{1655}: Absorption of band at 1655 cm^{-1}, A_{3450}: Absorption of band at 3450 cm^{-1}, and $A_{Band} = -\log$ (Transmittance).

2.3.3. X-ray diffraction (XRD)

At the Faculty of Pharmacy, Al-Azhar University in Cairo, Egypt, an X-ray diffractometer (Panalytical X'Pert Pro, Netherland) was used to examine the products for phase identification, purity, relative crystallinity, and crystallite size in the 2 θ range from 4 to 70° at a scanning speed of 2° min^{-1}. The radiation source was Cu−K, and the filter was nickel. According to Marei et al. [14], the following was done to get the crystalline index (CrI) values from the XRD data:

$$CrI_{110} = [(I_{110} - Iam) / I_{110}] \times 100$$

Where: I_{110}: maximum intensity at $2\theta \cong 20°$, and Iam: intensity of amorphous diffraction at $2\theta \cong 16°$.

2.3.4. Scanning electron microscopy (SEM)

The Regional Center of Mycology and Biotechnology at Al-Azhar University in Cairo, Egypt, used a scanning electron microscope (JEOL-JSM-5500 LV) in high vacuum mode to analyze chitosan's surface morphology and microstructure. The samples were air-dried in a CO_2 critical point drier before being placed on scanning electron microscope stubs (Tousimis Audosamdri-815). Gold was spat onto the surface for 30 s as part of the coating process in the SPI-Module. Between 10 and 20 KV, the samples were analyzed.

2.4. Biological bioassay

2.4.1. Cytotoxic activity of the prepared chitosan

The National Research Centre in Dokki, Giza, Egypt, provided HepG2, MCF-7, and WI-38 human liver cancer, breast cancer, and lung fibroblast cell lines. The cell lines were maintained at 37 °C in a humidified 5% CO_2 incubator with RPMI-1640 containing 10.0% fetal bovine serum (FBS), 100 μg/ml penicillin, and 100 μg/ml streptomycin. After incubation at 37 °C for 24 h, the samples dissolved in Dimethyl sulfoxide (DMSO) to a full monolayer sheet was formed in the 96-well tissue culture plate that had been injected with 1×10^5 cells/ml (100 μl/well). After the cells had produced a confluent sheet, the growth medium in the 96-well microtiter plates was drained, and the cell monolayer was washed twice with wash media. The material under examination was diluted by a factor of two in RPMI medium containing 2% serum (maintenance medium). Each dilution was evaluated at a concentration of 0.1 ml in separate wells, while three wells served as controls and received just maintenance medium. The plate was kept in a 37 °C incubator for analysis. Cells were examined for outward manifestations of toxicity, such as loss of monolayer, rounding, shrinkage, or granulation. Then, 5 mg/ml of phosphate-buffered saline (PBS) was used to make the MTT solution (BIO BASIC CANADA INC). Each well was supplemented with 20 μl of MTT solution. Mix the MTT into the medium by shaking the container at 150 rpm for 5 min After incubating the cells (at 37 °C with 5% carbon dioxide) for 1−5 h, various doses of chitosan (1000, 500, 250, 125, 62.5 and 31.25 μg/ml) were applied to determine how much MTT was metabolized. Get rid of your media. If any residue remains, wipe the plate with paper towels. Formazan, a byproduct of MTT metabolism, should be resuspended in 200 μl DMSO. Shake at 150 rpm for 5 min to fully incorporate the solvent into the formazan. Using an ELX-800 Biotek-USA ELISA reader, determine the optical density (OD) at 560 nm and remove the background at 620 nm. There must be a one-to-oe relationship between optical density and cell number [24].

The percentage of cell viability was calculated as
Cell viability (%) = (Mean OD of treated wells/Mean OD of control well) × 100

2.4.2. Anticoagulant assay: activated partial thromboplastin time (APTT)

The APTT test was performed according to the protocol described by Seedevi et al. [25]. Using a commercially available kit, the APTT value was calculated (Plasmatrol H-II, Liquicellin-E, BioMed). In this test, 10 μl of citrated blood plasma was combined with 25, 50 and 75 μg/ml of chitosan concentration in a glass vial and incubated at 37 °C for 1 h. After adding the 100 μl of Bovine Cephalin and incubating the mixture for 3 min at 37 °C, 0.25 mM of pre-heated $CaCl_2$ solution was added. At

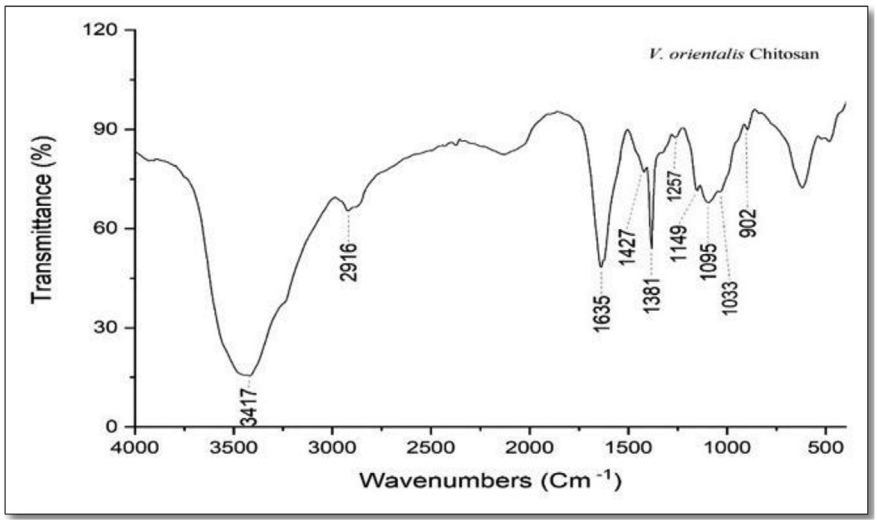

Fig. 1. The FT-IR spectra of the chitosan prepared from V. orientalis.

Al-Azhar University in Cairo, Egypt, the Regional Center of Mycology and Biotechnology measured and documented the clotting time.

2.4.3. Anticoagulant assay: Prothrombin Time (PT)

Chitosan's PT potential was determined using a technique similar to that described by Seedevi et al. [26]. After incubating the mixture at 37 °C for 10 min, 90 μl of citrated normal human plasma was added to 10 μl of (25, 50 and 75 μg/ml) chitosan. The clotting time was then measured at the Regional Center of Mycology and Biotechnology at Al-Azhar University in Cairo, Egypt, after combining 200 μl of PT reagent (after incubation).

2.5. Statistical analysis

All examinations were done in triplicates and the listed data are the average of the obtained results.

3. Results

3.1. Chitosan production and its preliminary identification

Adult *V. orientalis* and *A. thalassinus* were subjected to a range of processes, including deproteinization, demineralization, decolorization, and deacetylation, to extract chitosan. The confirmatory test showed that the chitin was successfully deacetylated into chitosan because the color changed from yellow to dark purple. Both *V. orientalis* and *A. thalassinus* had an 8.2% and 10.8% recovery rate for their chitosan, respectively.

3.2. Characterization of the extracted chitosan

3.2.1. Solubility test

The obtained chitosan powder was dissolved completely in 1.0% acetic acid within shake by hand,

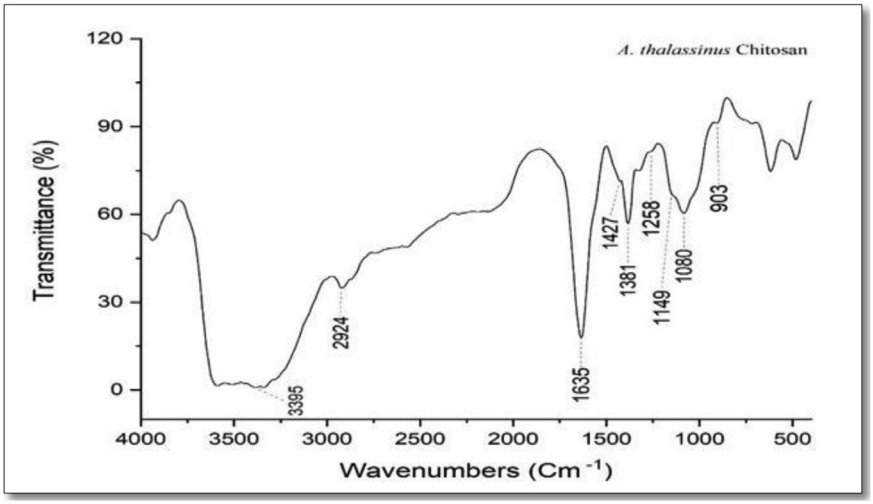

Fig. 2. The FT-IR spectra of the chitosan prepared from A. thalassinus.

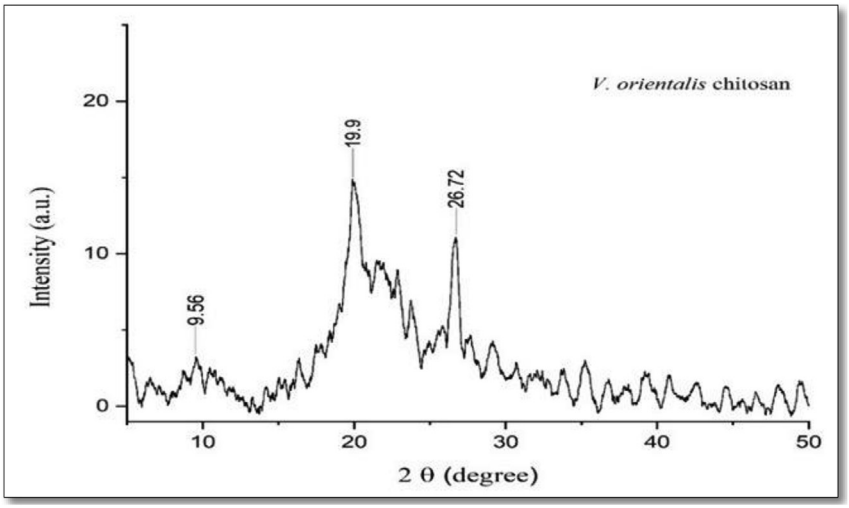

Fig. 3. The XRD pattern of chitosan extracted from V. orientalis.

indicating that samples have a degree of deacetylation above 50.0%.

3.2.2. Fourier transform infrared spectroscopy (FT-IR)

The wavelength range used in the FT-IR analysis of chitosan was 4000 to 400 cm^{-1}. A large, strong band at 3417 cm^{-1} was seen in the spectra of *V. orientalis* chitosan. This region corresponds to the stretching vibration of OH, the extension vibration of N−H, and the hydrogen bonds between sugar molecules. The asymmetric stretching vibration (CH_2) in the CH_2OH group was identified as the source of the 2916 cm^{-1} absorption bands. N-deacetylation was successful since an absorption peak in the amide I band (caused by −C═O stretching of a hydrogen-bonded −C═O−$NHCOCH_3$ group) appeared at about 1635 cm^{-1}. It was determined that the bands at 1427 and 1381 cm^{-1} originated from the symmetric bending (CH_3) in the $NHCOCH_3$ group and the bending (CH_2) in the CH_2OH group, respectively. The complex vibrations of the NHCO group were found to be associated with the wave number at 1257 cm^{-1} (Amide III band). At 1149 cm^{-1}, we analyzed the C−O−C symmetric stretching vibration in the glycosidic bond. The OH group's stretching vibration (C−O) was detected at 1095 cm^{-1}. The secondary OH group's stretching vibration (C−O) was detected at 1033 cm^{-1}. Also, the C−H out-of-plane vibration (Pyranose ring skeletal vibrations) was given the wave number of 902 cm-1 (Fig. 1). The chitosan extracted from *V. orientalis* showed a DDA of 73.74%.

A. thalassinus chitosan exhibited an absorption band at 3395 cm^{-1}, attributed to the stretching vibration of OH, the extension vibration of N−H, and

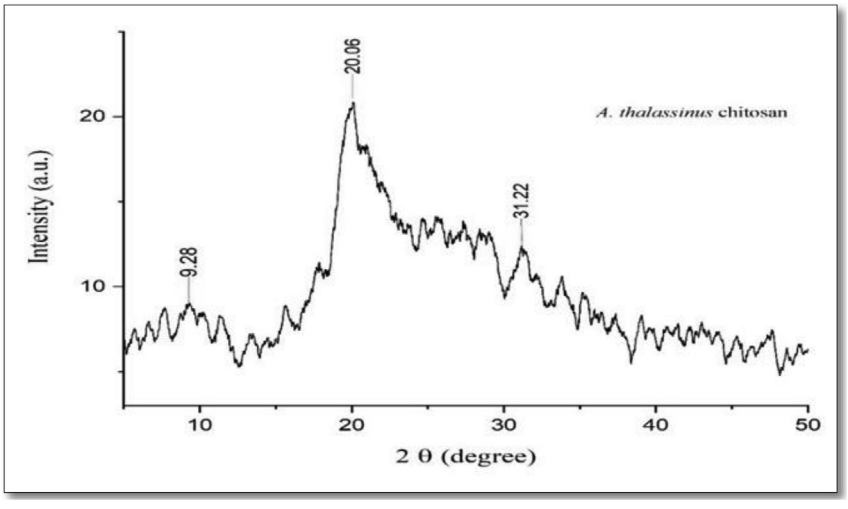

Fig. 4. The XRD pattern of chitosan extracted from A. thalassinus.

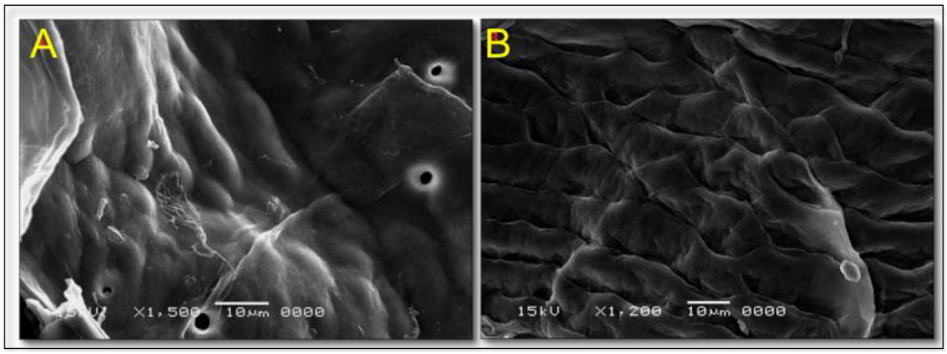

Fig. 5. The SEM images of chitosan from V. orientalis.

the hydrogen bonds between sugar molecules. Assigning the 2924 cm^{-1} absorption band to the CH_2OH group's asymmetric stretching vibration (CH_2) was challenging. N-deacetylation was successful since an absorption peak in the amide I band (caused by −C═O stretching of a hydrogen-bonded −C═O−$NHCOCH_3$ group) appeared at about 1635 cm^{-1}. It was determined that the bands at 1427 and 1381 cm^{-1} originated from the symmetric bending (CH_3) in the $NHCOCH_3$ group and the bending (CH_2) in the CH_2OH group, respectively. Complex NHCO group vibrations were found to be associated with the 1258 cm^{-1} wave number (Amide III band). At 1149 cm^{-1}, we analyzed the C−O−C symmetric stretching vibration in the glycosidic bond. At 1080 cm^{-1}, a C−O stretching vibration was detected in the OH group. The C−H out-of-plane vibration (Pyranose ring skeletal vibrations) was also attributed to the 903 cm^{-1} wave number (Fig. 2). *A. thalassinus* chitosan showed a DDA of 72.95%.

3.2.3. X-ray diffraction (XRD)

Two distinct peaks at about 19.9 and 26.72° were seen in the chitosan made by adult *V. orientalis*, and one weak Peak at 9.56° was seen in the X-ray diffraction measurements of the chitosan structures taken in the range of 2 = 4°−70° (Fig. 3). On the other hand, chitosan extracted from *A. thalassinus* exhibited one sharp Peak at 20.06° and two faint at 9.28 and 31.22° diffraction peaks (Fig. 4). The crystalline index (CrI) for *V. orientalis* chitosan was recorded at 53.8% vs. 77.7% by *A. thalassinus* chitosan.

3.2.4. Scanning electron microscopy (SEM)

An irregular masses and soft structure with some pores on its surface, rough surface sequentially fish scale shaped are observed for *V. orientalis* chitosan (Fig. 5a and b). Also, chitosan extracted from *A. thalassinus* showed interlaced structure, irregular block, and microfibrils parallel with voids (Fig. 6a and b).

3.3. Cytotoxic activity of the extracted chitosan

Data given in (Table 1, Figs. 7 and 8) showed cytotoxicity of *V. orientalis* and *A. thalassinus* extracted chitosan on MCF-7. The cellular viability revealed that a concentration of 1000 µg/ml from *V. orientalis* chitosan induced a drastic decrease in cellular viability with 17.99% cell viability, while 500 µg/ml induced 73.25% cell viability, and still increased till the concentration reached 125 µg/ml which showed 99.01% cell viability. The IC_{50} of *V. orientalis* chitosan recorded 706.22 µg/ml. Also, *A.*

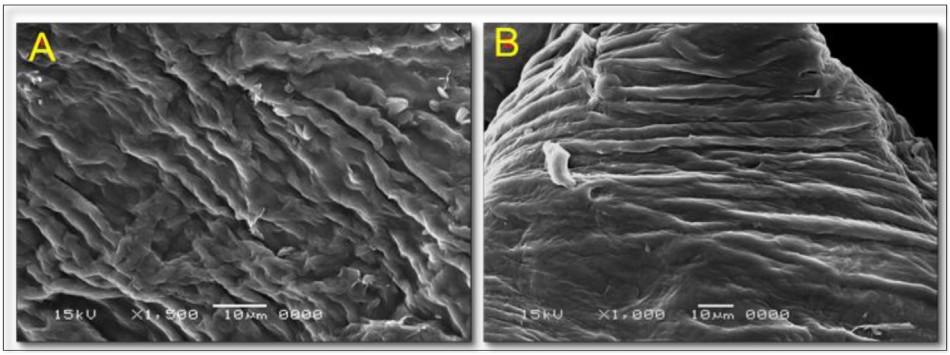

Fig. 6. The SEM images of chitosan from A. thalassinus.

Table 1. Cytotoxic activity for V. orientalis *and* A. thalassinus *chitosan against MCF-7 cell line.*

Chitosan	Conc. μg/ml	Optical density (O.D)			Mean O.D	Standard error (SE)	Viability %	Toxicity %	IC_{50} μg/ml
Control well	2:1	0.326	0.351	0.34	0.339 ± 0.01	0.007234	100	0	–
	1000	0.062	0.058	0.063	0.061 ± 0.002	0.001528	17.99410029	82.00589971	
	500	0.241	0.236	0.268	0.248 ± 0.01	0.009939	73.2546706	26.7453294	
	250	0.322	0.353	0.326	0.333 ± 0.0.1	0.009735	98.42674533	1.573254671	706.22
V. orientalis	125	0.347	0.331	0.329	0.335 ± 0.009	0.005696	99.01671583	0.983284169	
	62.5	0.335	0.336	0.327	0.332 ± 0.004	0.002848	98.13176008	1.868239921	
	31.25	0.346	0.321	0.35	0.339 ± 0.01	0.009074	100	0	
	1000	0.032	0.025	0.04	0.032 ± 0.007	0.004333	9.537856441	90.46214356	
	500	0.033	0.062	0.047	0.047 ± 0.01	0.008373	13.9626352	86.0373648	
A. thalassinus	250	0.124	0.092	0.106	0.107 ± 0.01	0.009262	31.66175025	68.33824975	188.78
	125	0.215	0.232	0.247	0.231 ± 0.01	0.009244	68.23992134	31.76007866	
	62.5	0.301	0.316	0.299	0.305 ± 0.009	0.005364	90.06882989	9.931170108	
	31.25	0.325	0.319	0.338	0.327 ± 0.009	0.005608	96.55850541	3.441494592	

thalassinus chitosan showed cytotoxicity on MCF-7, where cellular viability was recorded at 9.53 and 13.96% at 1000 and 500 μg/ml, respectively. The IC_{50} of *A. thalassinus* chitosan was 188.78 μg/ml.

Also, data in (Table 2, Figs. 9 and 10) illustrated the cytotoxicity of *V. orientalis* and *A. thalassinus* extracted chitosan against HepG2. The IC_{50} recorded 643.48 and 185.85 μg/ml for both *V. orientalis* and *A. thalassinus* extracted chitosan, respectively.

In addition, chitosan extracted from *V. orientalis* exhibited noncytotoxic effects at concentrations less than or equal to 250 μg/ml, while *A. thalassinus* chitosan showed no cytotoxic effects at concentrations ≤125 μg/ml against the WI-38 cell line (Table 3, Figs. 11 and 12).

3.4. Anticoagulant activity of the extracted chitosan

Results in (Table 4) exhibited that anticoagulant activity of *V. orientalis* extracted chitosan using APTT assay showed 38.28 ± 0.07, 45.38 ± 0.02 and 53.7 ± 0.01 s at 25, 50 and 75 μg/ml, respectively. While *A. thalassinus* chitosan reached 43.81 ± 0.02, 51.36 ± 0.01 and 58.91 ± 0.04 s at 25, 50 and 75 μg/ml, respectively. On the other hand, the anticoagulant activity of *V. orientalis* chitosan using PT assay recorded 12.16 ± 0.07 s at 25 μg/ml, compared with 14.37 ± 0.02 s for *A. thalassinus* chitosan at the same concentration. Accordingly, the results showed the anticoagulant potential of chitosan was weaker than the Heparin sodium salt (standard).

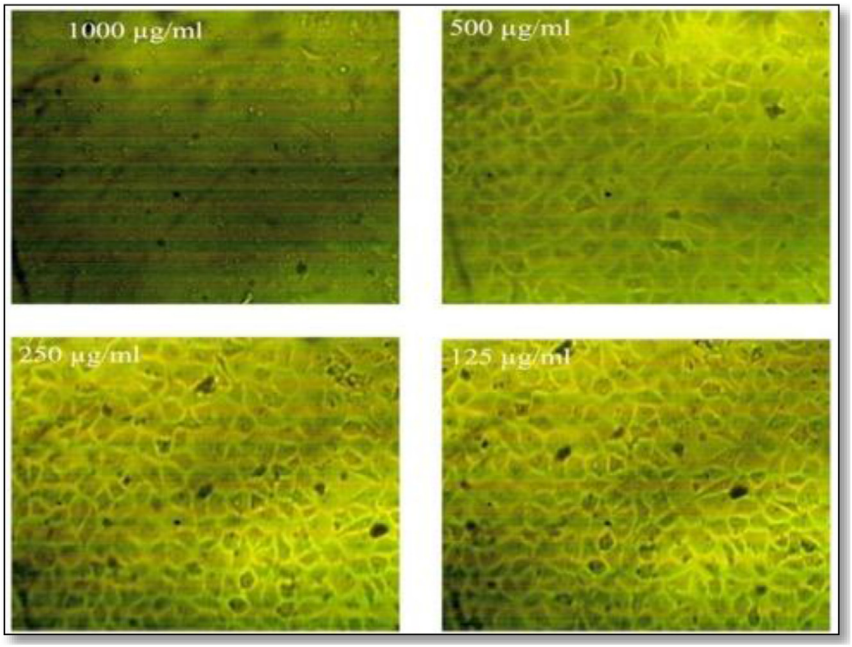

Fig. 7. Morphological changes of MCF-7 cell lines treated with V. orientalis *chitosan.*

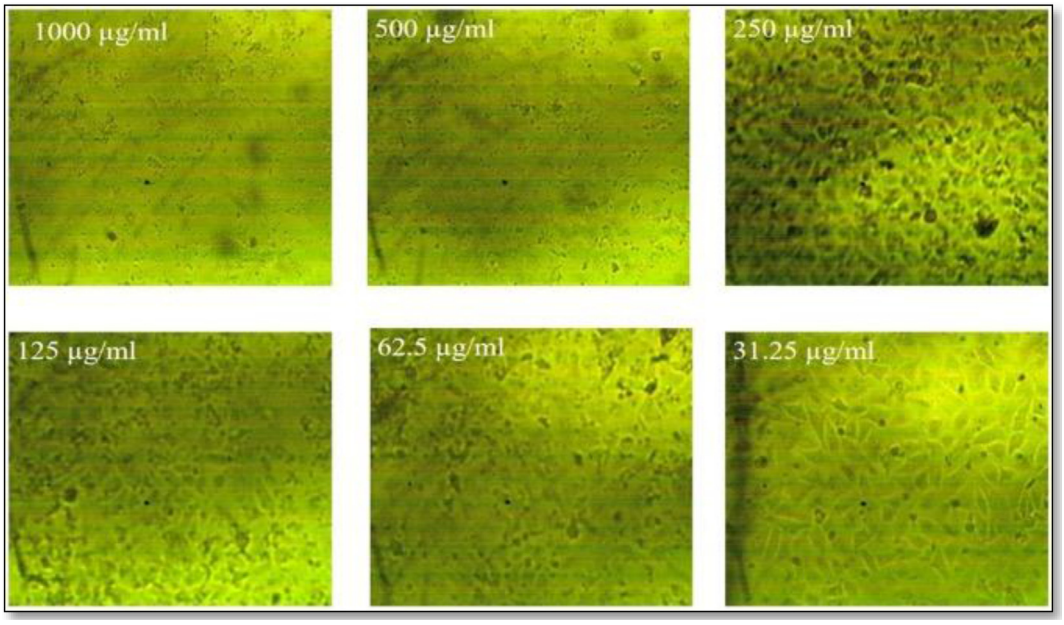

Fig. 8. Morphological changes of MCF-7 cell lines treated with A. thalassinus *chitosan.*

4. Discussion

The absorption peak of the amide I band (owing to −C═O stretching of hydrogen bound −C═O−NHCOCH$_3$ group) arises at roughly 1635 cm^{-1} for both *V. orientalis* and *A. thalassinus* isolated chitosan, as shown by Fourier transform infrared spectroscopy (FT-IR). These results agreed with the previously mentioned by Wanule et al. [27], who stated that FT-IR Spectra for chitosan derived from *Periplaneta americana* showed a peak at 3400 cm^{-1}, indicating symmetric stretching vibration of OH and amine N−H 2923.88 cm^{-1} indicate the presence of CH stretch, 1650.95 was due to C═O stretching (amide I) 1095.49 and 1033.77 peaks for C−O stretching and Peak at 894.91 is a ring stretching a characteristic bond for β-1-4 glycosidic linkage. Also, chitosan extracted from *V. orientalis* adults recorded the highest degree of deacetylations (DDA) (73.74%), compared with *A. thalassinus* extracted chitosan (DDA: 72.95%). Similar results were recorded by Battampara et al. [28], where the DDA% of chitosan derived from silkworm pupae was 67.0%, compared with 59.0% for the eggshell chitosan, maximum DDA % of chitosan isolated from shrimp (*Panaeus monodon*), crab (*Scylla olivicea* and *Scylla serrata*), locust (*Schistocerca gregaria*), honeybee (*Apis mellifera*), beetle (*Calosoma rugosa*), and fish scales (*Labeo rohita*) was 95.0−98.0% [16].

In addition, The X-ray diffraction (XRD) measurements also showed two sharp peaks for chitosan extracted from *V. orientalis* at approximately 19.9 and 26.72° and one faint peaks at 9.56°. While chitosan extracted from *A. thalassinus* exhibited one sharp

Table 2. Cytotoxic activity for V. orientalis *and* A. thalassinus *chitosan against HepG2 cell line.*

Chitosan	Conc. µg/ml	Optical density (O.D)			Mean O.D	Standard error (SE)	Viability %	Toxicity %	IC_{50} µg/ml
Control well	2:1	0.346	0.362	0.342	0.35 ± 0.01	0.00611	100	0	−
	1000	0.085	0.072	0.069	0.075 ± 0.008	0.00491	21.52380952	78.47619048	
	500	0.186	0.194	0.197	0.192 ± 0.005	0.003283	54.95238095	45.04761905	
	250	0.287	0.301	0.316	0.301 ± 0.01	0.008373	86.0952381	13.9047619	643.48
V. orientalis	125	0.358	0.339	0.35	0.349 ± 0.009	0.005508	99.71428571	0.285714286	
	62.5	0.338	0.359	0.351	0.349 ± 0.01	0.006119	99.80952381	0.19047619	
	31.25	0.342	0.338	0.352	0.344 ± 0.007	0.004163	98.28571429	1.714285714	
	1000	0.062	0.044	0.053	0.053 ± 0.009	0.005196	15.14285714	84.85714286	
	500	0.084	0.062	0.072	0.072 ± 0.01	0.00636	20.76190476	79.23809524	
	250	0.092	0.108	0.113	0.104 ± 0.01	0.006333	29.80952381	70.19047619	
A. thalassinus	125	0.245	0.236	0.228	0.236 ± 0.008	0.00491	67.52380952	32.47619048	185.85
	62.5	0.315	0.328	0.326	0.323 ± 0.007	0.004041	92.28571429	7.714285714	
	31.25	0.351	0.344	0.352	0.349 ± 0.004	0.002517	99.71428571	0.285714286	

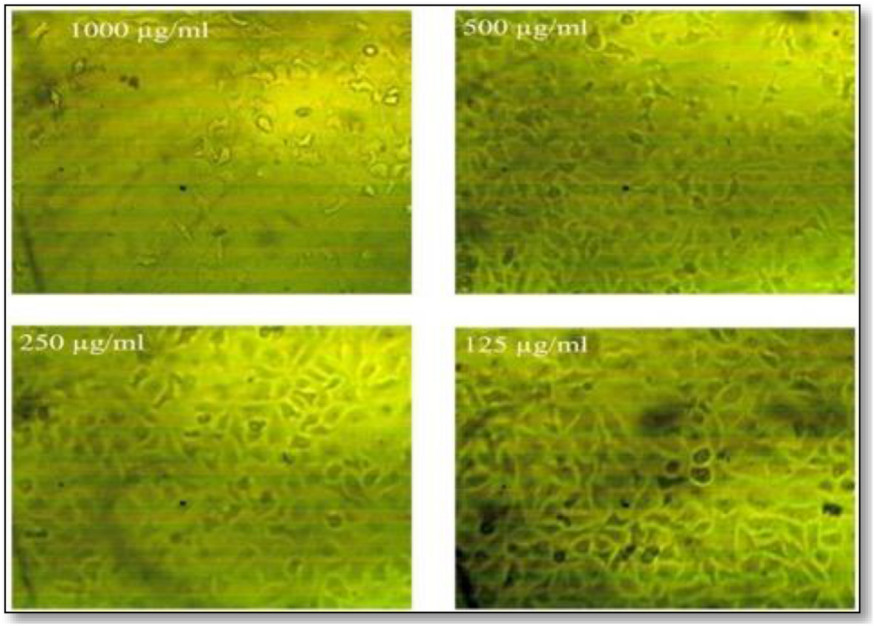

Fig. 9. Morphological changes of HepG2 cell lines treated with V. orientalis *chitosan.*

peaks at 20.06° and two faint at 9.28 and 31.22° diffraction peaks. The crystalline index (CrI) for *V. orientalis* chitosan was recorded at 53.8% vs. 77.7% recorded by *A. thalassinus* chitosan, respectively. These findings are consistent with those of [29], which found that chitosan from silkworm pupae had a crystallinity of 48.0% compared to 38.0% from egg shells [28], and which used XRD to illustrate differentiation between chitin and chitosan derived from *Tenebrio molitor* cuticle [30].

Scanning Electron Microscopy (SEM) showed irregular masses and a soft structure with some pores on its surface; rough surface sequentially fish scale shaped are observed for *V. orientalis* chitosan.

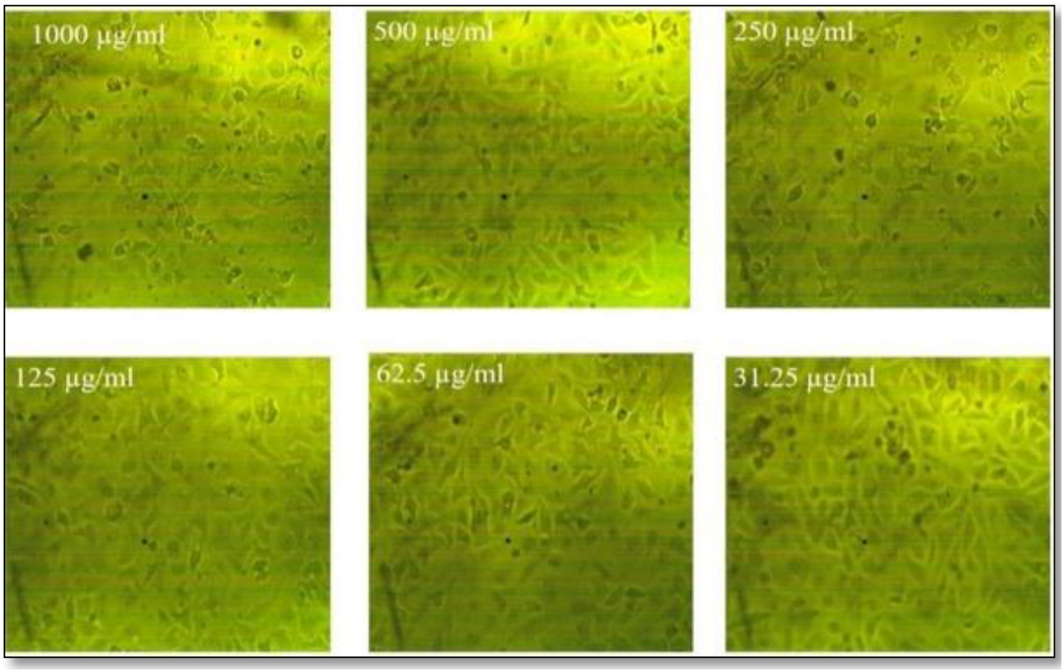

Fig. 10. Morphological changes of HepG2 cell lines treated with A. thalassinus *chitosan.*

Table 3. Cytotoxic activity for V. orientalis *and* A. thalassinus *chitosan against WI-38 cell line.*

Chitosan	Conc. μg/ml			Optical density (O.D)	Mean O.D	Standard error (SE)	Viability %	Toxicity %
Control well	2:1	0.371	0.383	0.386	0.38 ± 0.007	0.004583	100	0
	1000	0.083	0.091	0.108	0.094 ± 0.01	0.007371	24.73684211	75.26315789
	500	0.289	0.312	0.307	0.302 ± 0.01	0.006984	79.64912281	20.35087719
	250	0.384	0.374	0.388	0.382 ± 0.007	0.004163	100.5263158	0
V. orientalis	125	0.375	0.388	0.38	0.381 ± 0.006	0.003786	100.2631579	0
	62.5	0.369	0.392	0.384	0.381 ± 0.01	0.006741	100.4385965	0
	31.25	0.39	0.372	0.379	0.380 ± 0.009	0.005239	100.0877193	0
	1000	0.095	0.105	0.106	0.102 ± 0.006	0.003512	26.84210526	73.15789474
	500	0.241	0.216	0.235	0.230 ± 0.01	0.007535	60.70175439	39.29824561
A. thalassinus	250	0.314	0.325	0.336	0.325 ± 0.01	0.006351	85.52631579	14.47368421
	125	0.384	0.372	0.373	0.376 ± 0.006	0.003844	99.03508772	0.964912281
	62.5	0.388	0.386	0.374	0.382 ± 0.007	0.004372	100.7017544	0
	31.25	0.362	0.394	0.382	0.379 ± 0.01	0.009333	99.8245614	0.175438596

Also, chitosan extracted from *A. thalassinus* showed interlaced structure, irregular block, and microfibrils parallel with voids. In agreement with the present results, **Kaya** et al. [31] reported that SEM studies of chitosan extracted from *Leptinotarsa decemlineata* larva and adult revealed that these structures consisted of nanofibers, **Marei** et al. [14] found that SEM analysis of chitosan extracted from different local sources (shrimp, *Penaeus monodon;* desert locust, *S. gregaria;* honey bee, *A. mellifera,* and beetles, *C. rugosa*) indicated dense nanofibers surface structure of shrimp, locust and beetle chitosan and hard rough surface of honey bee chitosan and **Aloucheh** et al., [32] recorded that, chitosan from the aquatic beetles (Hydraenidae) is segregated chitosan has a smooth surface with amorphous property according to the SEM images.

Obtained data of cytotoxic activity of both extracted chitosan samples revealed that the cellular viability of the MCF-7 cell line recorded at 17.99 and 9.53% by *V. orientalis* and *A. thalassinus* extracted chitosan at 1000 μg/ml, respectively. In addition, at 500 μg/ml, the viability of the HepG2 cell line was recorded 54.95 and 20.76% by *V. orientalis* and *A. thalassinus*, respectively. On the other hand, *V. orientalis* and *A. thalassinus* extracted chitosan showed

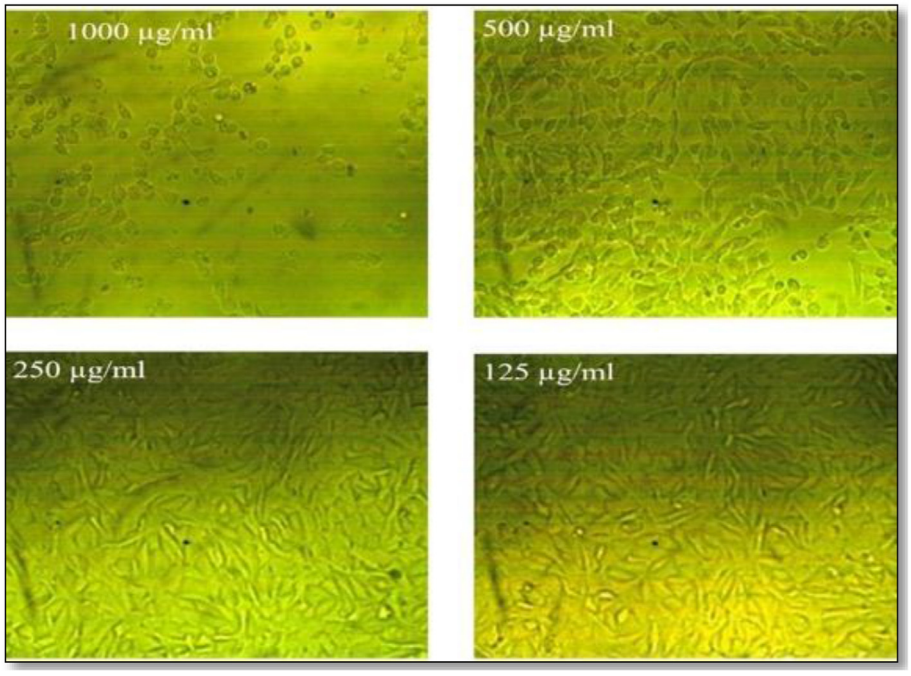

Fig. 11. Morphological changes of WI-38 cell lines treated with V. orientalis *chitosan.*

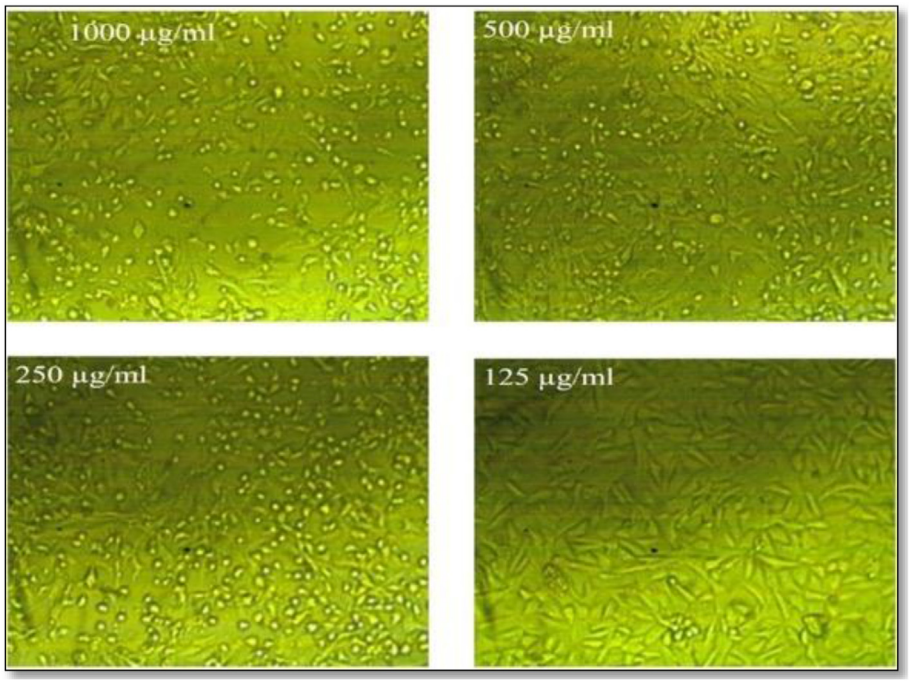

Fig. 12. Morphological changes of WI-38 cell lines treated with A. thalassinus *chitosan.*

noncytotoxic effects against the WI-38 cell line at concentrations less than or equal to 250 and 125 µg/ml, meaning their side effects are low. These findings are consistent with those of Ai et al. [33], who found that chitosan extracted from *Musca domestica* housefly larvae inhibited the growth of human cervical carcinoma (HeLa) and mouse sarcoma-180 (S-180) tumor cell lines in vitro at doses as low as 1.0 mg/mL (50.8 and 52.9% inhibition, respectively), and with those of [10], who studied the anticancer activity of chitosan prepared from The American cockroach against HepG2 and MCF-7 cell lines and reported that cytotoxicity has a positive relationship with the chitosan concentration, IC_{50} values were recorded 329 and 195 µg/ml, respectively.

Results showed that anticoagulant activity of *V. orientalis* and *A. thalassinus* extracted chitosan using APTT assay recorded 53.7 ± 0.01 and 58.91 ± 0.04 s at 75 µg/ml, compared with 115.1 ± 0.01 s for heparin sodium salt. Also, the anticoagulant activity of *V. orientalis* chitosan using PT assay was recorded at 12.16 ± 0.07 s at 25 µg/ml, compared with 14.37 ± 0.02 s for *A. thalassinus* chitosan at the same concentration, respectively. Both studies showed that extracted chitosan had a lesser anticoagulant capability than heparin and required a greater dosage to match that of the commercial anticoagulant (Heparin sodium salt) (APTT and PT). These results are in consistent with the previously recorded results by Arasukumar et al. [34], who employed APTT and PT tests to investigate the anticoagulant activity of chitosan derived from *Thenus unimaculatus*, using heparin sodium as the reference standard, anticoagulant activity of *T. unimaculatus* chitosan was recorded at 49.7 and 20.9 s at 50 µg/ml by APTT and PT assays, respectively. Compared with 61.2 and 31.4 s recorded by heparin, respectively, and [35] who reported that

Table 4. Anticoagulant activity of extracted chitosan and heparin based on APTT and PT assays.

Assay	Conc. µg/ml	Anticoagulant Values in sec. caused by chitosan		Heparin sodium salt (standard)
		V. orientalis	*A. thalassinus*	
Activated partial thromboplastin time (APTT)	25	38.28 ± 0.07	43.81 ± 0.02	61.2 ± 0.07
	50	45.38 ± 0.02	51.36 ± 0.01	84.5 ± 0.01
	75	53.7 ± 0.01	58.91 ± 0.04	115.1 ± 0.01
Prothrombin time (PT)	25	12.16 ± 0.07	14.37 ± 0.02	26.49 ± 0.01
	50	14.57 ± 0.03	14.83 ± 0.02	39.19 ± 0.01
	75	18.86 ± 0.03	17.23 ± 0.02	51.59 ± 0.01

anticoagulant activity of the different types of blue crab chitosan recorded 31.2, 14.8 and 14.4 s using APTT, Quick time (QT), and thrombin time (TT), respectively in vitro assays.

4.1. Conclusion

Chitosan were successfully produced from *V. orientalis* and *A. thalassinus* adults, the yield of chitosan were recorded 8.2 and 10.8%, respectively, and showed a DDA% 73.74 and 72.95%, respectively. The (CrI) recorded 53.8% for *V. orientalis* chitosan vs. 77.7% by *A. thalassinus* chitosan. Both extracted chitosan can be a potential natural compound for the treatment of tumor cells (MCF-7 and HepG2). Also, *V. orientalis* and *A. thalassinus* exhibited anticoagulant potential depended on concentrations in APTT and PT assays. From the results of the present study, the chitosan can be used as a promising anticoagulant activity and anticancer agents, to be applied in biomedical applications due to its nontoxic nature.

Conflicts of interest

The authors have no conflicts of interest regarding this investigation.

References

[1] Kumar MNVR. A review of chitin and chitosan applications. React Funct Polym 2000;46:1−27. https://doi.org/10.1016/S1381-5148(00)00038-9.

[2] Rinaudo M. Chitin and chitosan: properties and applications. Prog Polym Sci 2006;31:603−32. https://doi.org/10.1016/j.progpolymsci.2006.06.001.

[3] El-Mehdawy AA, Koriem M, Amin RM, Shehata AZI, El-Naggar HA. Green synthesis of silver nanoparticles using chitosan extracted from Penaeus indicus and its potential activity as an aquatic larvicidal agent of Culex pipens. Egypt J Aquat Biol Fish 2022;26:425−42. https://doi.org/10.21608/ejabf.2022.219887.

[4] Xia WS. Physiological activities of chitosan and its application in functional foods. J Chin Inst Food Sci Technol 2003;3:77−81. https://www.researchgate.net/publication/304424772.

[5] Struszczyk MH. Chitin and chitosan − part III. Some aspects of biodegradation and bioactivity. Polimery 2002;47:619−29. https://ichp.vot.pl/index.php/.

[6] Ruoslahti E, Bhatia SN, Sailor MJ. Targeting of drugs and nanoparticles to tumors. J Cell Biol 2010;188:759−68. https://doi.org/10.1083/jcb.200910104.

[7] Anna B, Solaiman D, Alexey S, Sali D. Pharmacological and biological effects of chitosan. Res J Pharm Technol 2020;13:1043−9. https://doi.org/10.5958/0974-360X.2020.00192.4.

[8] Liu W, Sun S, Cao Z, Zhang X, Yao K, Lu WW, et al. An investigation on the physicochemical properties of chitosan/DNA polyelectrolyte complexes. Biomaterials 2005;26:2705−11. https://doi.org/10.1016/j.biomaterials.2004.07.038.

[9] Torre LA, Bray F, Siegel RL, Ferlay J, Lortet-Tieulent J, Jemal A. Global cancer statistics. CA A Cancer J Clin 2015;65:87−108. https://doi.org/10.3322/caac.21262.

[10] Mahboub MT, Hassan MI, Bream AS, Mohamed AF, Abdel-Samad MRK. Preparation, characterization and anticancer activity of chitosan prepared from the American cockroach, Periplaneta Americana. Egypt Acad J Biol Sci 2021;14:163−71. https://doi.org/10.21608/eajbsa.2021.185450.

[11] Sajomsang W, Gonil P. Preparation and characterization of α-chitin from cicada sloughs. Mater Sci Eng C 2010;30:357−63. https://doi.org/10.1016/j.msec.2009.11.014.

[12] Liu S, Sun J, Yu L, Zhang C, Bi J, Zhu F, et al. Extraction and characterization of chitin from the beetle Holotrichia parallela Motschulsky. Molecules 2012;17:4604−11. https://doi.org/10.3390/molecules17044604.

[13] Hassan MI, Taher FA, Mohamed AF, Kamel MR. Antimicrobial activities of chitosan nanoparticles prepared from Lucilia Cuprina Maggots (Diptera: calliphoridae). J Egypt Soc Parasitol 2016;46:563−70. https://doi.org/10.21608/jesp.2016.88258.

[14] Marei NH, Abd El Samiee E, Salah T, Saad GR, Elwahy AHM. Isolation and characterization of chitosan from different local insects in Egypt. Int J Biol Macromol 2016;82:871−7. https://doi.org/10.1016/j.ijbiomac.2015.10.024.

[15] Kim MW, Song YS, Han YS, Jo YH, Choi MH, Park YK, et al. Production of chitin and chitosan from the exoskeleton of adult two-spotted field crickets (Gryllus bimaculatus). Entomol Res 2017;47:279−85. https://doi.org/10.1111/1748-5967.12239.

[16] Ibram A, Ionescu AM, Cadar E. Comparison of extraction methods of chitin and chitosan from different sources. Eur J Med Sci 2021;5:44−56. https://revistia.org/files/articles/ejnm_v2_i2_19/Ibram.pdf.

[17] Chernysh S, Kim SI, Bekker G, Pleskach VA, Filatova NA, Anikin VB, et al. Antiviral and antitumor peptides from insects. Proc Natl Acad Sci USA 2002;99:12628−32. https://doi.org/10.1073/pnas.192301899.

[18] Amer MS, Hammad KM, Hasaballah AI, Shehata AZI, Saeed MS. Effectiveness evaluation of Chrysomya albiceps (Diptera: calliphoridae) and Musca domestica (Diptera: muscidae) maggots extracts as antimicrobial and antiviral agent. Egypt J Aquat Biol Fish 2019;23:561−73. https://doi.org/10.21608/ejabf.2019.48643.

[19] Gobinath T, Thamizhselvan S, Ramakrishnan A, Ravichandran S. Preparation and characterization of chitosan from Perna viridis (Linnaeus, 1758) shell waste as raw material. Res J Pharm Technol 2021;14:2757−62. https://doi.org/10.52711/0974-360X.2021.00486.

[20] Badman J, Harrison JF, McGarry MP. Grasshoppers in research and education: methods for maintenance and production. Lab Anim 2007;36:27−31. https://doi.org/10.1038/laban0307-27.

[21] Kaya M, Baran T, Ozusaglam MA, Cakmak YS, Tozak KO, Mol A, et al. Extraction and characterization of chitin and chitosan with antimicrobial and antioxidant activities from cosmopolitan Orthoptera species (Insecta). Biotechnol Bioproc Eng 2015;20:168−79. https://doi.org/10.1007/s12257-014-0391-z.

[22] Islam MM, Masum SM, Rahman MM, Molla MAI, Shaikh AA, Roy SK. Preparation of chitosan from shrimp shell and investigation of its properties. Int J Basic Appl Sci 2011;11:77−80.

[23] Akila RM. Fermentative production of fungal Chitosan, a versatile biopolymer (perspectives and its applications). Adv Appl Sci Res 2014;5:157−70.

[24] Ciapetti G, Cenni E, Pratelli L, Pizzoferrato A. In vitro evaluation of cell/biomaterial interaction by MTT assay. Biomaterials 1993;14:359−64. https://doi.org/10.1016/0142-9612(93)90055-7.

[25] Seedevi P, Moovendhan M, Viramani S, Shanmugam A. Bioactive potential and structural characterization of sulphated polysaccharide from seaweed (Gracilaria corticata). Carbohydr Polym 2017;155:516−24. https://doi.org/10.1016/j.carbpol.2016.09.011.

[26] Seedevi P, Moovendhan M, Sudharsan S, Vasanthkumar S, Srinivasan A, Vairamani S, et al. Structural characterization and bioactivities of sulfated polysaccharide from Monostroma oxyspermum. Int J Biol Macromol 2015;72:1459−65. https://doi.org/10.1016/j.ijbiomac.2014.09.062.

[27] Wanule D, Balkhande JV, Ratnakar PU, Kulkarni AN, Bhowate CS. Extraction and FTIR analysis of chitosan from American cockroach, Periplaneta americana. Int j eng Innov

Technol 2014;3:299−304. https://www.researchgate.net/publication/269285580.
[28] Battampara P, Sathish TN, Reddy R, Guna V, Nagananda GS, Reddy N, et al. Properties of chitin and chitosan extracted from silkworm pupae and egg shells. Int J Biol Macromol 2020;161:1296−304. https://doi.org/10.1016/j.ijbiomac.2020.07.161.
[29] Rady MH, Essa EE, Mamoun SAM, Momen SAA, Salama MS, Barakat EMS, et al. Characterization and solubilization of chitosan from the oriental hornet (Vespa orientalis). J Egypt Soc Parasitol 2018;48:669−76. https://doi.org/10.21608/jesp.2018.76586.
[30] Silva-Lucas AJ, Oreste EQ, Costa HLG, López HM, Saad CDM, Prentice C. Extraction, physicochemical characterization and morphological properties of chitin and chitosan from cuticles of edible insects. Food Chem 2021;343:128550. https://doi.org/10.1016/j.foodchem.2020.128550.
[31] Kaya M, Baran T, Erdogan S, Mentes A, Ozusağlam MA, Çakmak YS. Physicochemical comparison of chitin and chitosan obtained from larvae and adult Colorado potato beetle (Leptinotarsa decemlineata). Mater Sci Eng C 2014;45:72−81. https://doi.org/10.1016/j.msec.2014.09.004.
[32] Aloucheh RM, Baris O, Asadi A, Golamzadeh S, Sadeghi MK. Characterization of aquatic beetles shells (Hydraenidae family) derived chitosan and its application in order to eliminate the environmental pollutant bacteria. Anthropog Pollut J 2019;3:43−8. https://doi.org/10.22034/ap.2019.668483.
[33] Ai H, Wang F, Yang Q, Zhu F, Lei C. Preparation and biological activities of chitosan from the larvae of housefly, Musca domestica. Carbohydr Polym 2008;72:419−23. https://doi.org/10.1016/j.carbpol.2007.09.010.
[34] Arasukumar B, Prabakaran G, Gunalan B, Moovendhan M. Chemical composition, structural features, surface morphology and bioactivities of chitosan derivatives from lobster (Thenus unimaculatus) shells. Int J Biol Macromol 2019;135:1237−45. https://doi.org/10.1016/j.ijbiomac.2019.06.033.
[35] Hamdi M, Nasri R, Ben-Amor I, Li S, Gargouri J, Nasri M. Structural features, anti-coagulant and anti-adhesive potentials of blue crab (Portunus segnis) chitosan derivatives: study of the effects of acetylation degree and molecular weight. Int J Biol Macromol 2020;160:593−601. https://doi.org/10.1016/j.ijbiomac.2020.05.246.